Molecular Crystals and Liquid Crystals

ISSN: 1542-1406 (Print) 1563-5287 (Online) Journal homepage: http://www.tandfonline.com/loi/gmcl20

Synthesis, characterization and photovoltaic properties of low band gap donor-acceptor polymers containing benzodithiophene donor unit with fluorenylthiophene as 2D-conjugated side for organic solar cell application

Taeik Kim, Nallan Chakravarthi, Gunasekar Kumarasamy & Sung-Ho Jin

To cite this article: Taeik Kim, Nallan Chakravarthi, Gunasekar Kumarasamy & Sung-Ho Jin (2016) Synthesis, characterization and photovoltaic properties of low band gap donor-acceptor polymers containing benzodithiophene donor unit with fluorenylthiophene as 2D-conjugated side for organic solar cell application, Molecular Crystals and Liquid Crystals, 635:1, 45-56, DOI: 10.1080/15421406.2016.1199999

To link to this article: http://dx.doi.org/10.1080/15421406.2016.1199999

MOLECULAR CRYSTALS AND LIQUID CRYSTALS
2016, VOL. 635, 45–56
http://dx.doi.org/10.1080/15421406.2016.1199999

Taylor & Francis
Taylor & Francis Group

Synthesis, characterization and photovoltaic properties of low band gap donor-acceptor polymers containing benzodithiophene donor unit with fluorenylthiophene as 2D-conjugated side for organic solar cell application

Taeik Kim, Nallan Chakravarthi, Gunasekar Kumarasamy, and Sung-Ho Jin

Department of Chemistry Education, Graduate Department of Chemical Materials, BK21 PLUS Team for Advanced Chemical Materials, and Institute for Plastic Information and Energy Materials, Pusan National University, Busan, Republic of Korea

ABSTRACT

Two donor−acceptor low band gap polymers P1 (octyl as solubilizing group) and P2 (ethylhexyl as solubilizing group) containing fluorenylthiophene-substituted benzoditihiophene as an electron-rich unit and 3,6-bis(5-bromothiophen-2-yl)-2,5-bis(2-ethylhexyl)pyrrolo[3,4-c]pyrrole-1,4(2H,5H)-dione as an electron-deficient unit are designed and synthesized for polymer solar cells application. Compared with P2 based on ethyl hexyl group, P1 with octyl group displays well resolved vibronic shoulder peak in absorption spectra, stronger intermolecular interactions, and higher hole mobility. Polymer solar cells based on P1 and [6,6]-phenyl-C_{71}-butyric acid methyl ester ($PC_{71}BM$) exhibit a maximum power conversion efficiency of 1.78% under AM 1.5G illumination (100 mW/cm^2).

KEYWORDS

Bulk heterojunction solar cells; low-band gap polymers; benzodithiophene; π-conjugated polymer

Introduction

The donor-acceptor low band gap (LBG) polymers for bulk heterojunction (BHJ) polymer solar cells (PSCs) based on p-type conjugated polymers as donors and n-type fullerene derivatives as acceptors have intensively attracted attention due to their advantages of light weight, low cost, easy fabrication, and the potential of flexible large-area devices[1]. The key parameter in PSCs is the power conversion efficiency (PCE) of the devices. The factors that related to the PCEs of the PSCs are the open-circuit voltage (V_{oc}), short-circuit current (J_{sc}), and fill factor (FF)[2]. V_{oc} is limited by the difference between the highest occupied molecular orbital (HOMO) of the donor and the lowest unoccupied molecular orbital (LUMO) of the acceptor[3]. The J_{sc} is closely related to the absorption capacity and charge-carrier mobility of the photovoltaic materials, and the FF is influenced by the charge-carrier mobility of the photoactive layer. Higher charge-carrier mobility results in larger J_{sc} and higher FF values[4]. In order to achieve high PCEs, it is a proven fact that the polymer donor with ideal properties in PSCs should exhibit strong and broad absorption with high absorption coefficient, high charge-carrier mobility, appropriate molecular energy levels for matching with the fullerene

CONTACT Sung-Ho Jin shjin@pusan.ac.kr Department of Chemistry Education, Graduate Department of Frontier Materials Chemistry, and Institute for Plastic Information and Energy Materials, Pusan National University, Busan 609-735, Korea.
Color versions of one or more of the figures in the article can be found online at www.tandfonline.com/gmcl.

derivatives[5]. In order to improve the visible absorption and decrease HOMO energy level of the conjugated polymers, extensive effort has focused on developing donor-acceptor conjugated polymers. With this strategies, recently PCEs over 10% have been reported for both single and multi-junction organic solar cells[6].

Benzodithiophene (BDT) skeleton has been extensively applied as a donor unit in π-conjugated polymers for the reason of its highly planar nature and inclined to provide a simple way to attach several conjugate side chain groups to further improve the backbone planarity and modulate the energy levels[7]. With the intention of improving the PCE of BDT based π-conjugated polymers, various groups on the central phenyl ring of the BDT unit were introduced. This structural alteration led to PCEs of above 10%[8]. The combination of fluorene and thiophene units, which is the important functionality to enhance the molecular assembly in the small molecular based liquid crystalline materials, has not so far introduced on the central phenyl ring of BDT for BHJ PSCs[9]. Further, it is well proven that the size and topology (e.g., linear, branched) of the alkyl side chains affixed to the five membered aromatic heterocycle moiety also influence the planarity, morphology, and photovoltaic parameters of the resultant polymers[10]. In this contribution, we designed and synthesized two donor-acceptor LBG polymers containing thienofluorene (FlT) linked benzodithiophene (FlT-BDT) as donor unit and 3,6-bis(5-bromothiophen-2-yl)-2,5-bis(2-ethylhexyl)pyrrolo[3,4-c]pyrrole-1,4(2H,5H)-dione (DPP) as acceptor unit. Here, we introduced FlT as a new side chain group substituent perpendicular to the BDT unit in upward and downward directions. The conjugated FlT substituents vertical to the polymer backbone is also expected to provide a broader absorption in the visible region. Furthermore, by introducing this entity in donor-acceptor structures, a deeper HOMO energy level can be attained, which is predicted to generate higher V_{oc} values in BHJ PSCs[11]. Additionally, we anticipate that the variation in alkyl chain (octyl vs 2-ethylhexyl) will have significant impact on the charge carrier mobility and PCEs.

Experimental

General information

All the chemicals and reagents purchased from Sigma-Aldirich were used without any further purification. Polymerization was performed in a CEM-focused microwave TM synthesis system. The number-average molecular weight (M_n) and polydispersity index (PDI) of the polymers were determined by gel permeation chromatography (GPC) using a PL gel 5 μm MLXED-C column on an Agilent 1100 series liquid chromatography system with THF as an eluent and calibration with polystyrene standards. ^{1}H and ^{13}C NMR spectra were recorded in $CDCl_3$ on a Varian Mercury 300 using tetramethylsilane as an internal reference. Thermogravimmetric analysis (TGA) was obtained with Mettler Toledo TGA/SDTA 851e under an N_2 atmosphere at a heating rate of 10°C/min, respectively. The UV-visible absorption spectra were measured using a Jasco V-570 UV-visible spectrometer. The cyclic voltammetry (CV) analysis was carried out in a 0.1 M solution of tetrabutylammonium perchlorate in anhydrous acetonitrile at a scan rate of 100 mV/s using a CHI 600C potentiostat, a three-electrode cell with platinum electrode as the working electrode, Ag/AgCl as the reference electrode, and a platinum (Pt) wire as the counter electrode. Polymer thin films were coated on the Pt electrode and dried before the experiment. 2-(9,9-dioctyl-9H-fluoren-2-yl)thiophene (FlT-OC) and 2-(9,9-bis(2-ethylhexyl)-9H-fluoren-2-yl)thiophene (FlT-EH) were prepared according to the reported procedures[9].

Synthesis of 4,8-bis(5-(9,9-dioctyl-9H-fluoren-2-yl)thiophen-2-yl)benzo[1,2-b:4,5-b′] dithiophene (FlT-BDT-OC)

FlT-OC (2.00 g, 4.23 mmol) was dissolved in dry tetrahydrofuran (THF) and the mixture was cooled to −78°C. 2.5 M n-BuLi in hexane (1.69 mL, 4.23 mmol) was slowly added to the solution and the reaction mixture was stirred for 1 h at 60°C. After cooling to room temperature, benzo[1,2-b:4,5-b′]dithiophene-4,8-dione (0.42 g, 1.92 mmol) was added quickly, and then heated to 60°C for 2 h. The dark red solution was cooled to room temperature again, tin chloride anhydrate dissolved in 20% HCl solution was added, and then the reaction was heated to 60°C for 2 h. The reaction was diluted with ether, and the organic layer was washed with water, dried with Na_2SO_4, filtered, the solvent was removed under reduced pressure and purified by silica gel column chromatography using dichloromethane(MC) as an eluent to afford a yellowish solid (0.89 g, yield: 42%). ^{1}H NMR (300 MHz, $CDCl_3$): δ (ppm) 7.80–7.66 (m, 10H), 7.59–7.50 (m, 6H), 7.40–7.29 (m, 6H), 2.04–1.93 (m, 8H), 1.29–0.94 (m, 40H), 0.81 (t, 6H), 0.73–0.60 (m, 4H). ^{13}C NMR (75 MHz, $CDCl_3$): δ (ppm) 151.6, 150.9, 146.1, 141.0, 140.7, 139.1, 138.5, 136.6, 132.7, 129.2, 127.8, 127.2, 126.8, 124.7, 123.8, 123.3, 123.1, 122.8, 120.1, 119.9, 119.7, 55.2, 40.4, 31.8, 30.0, 29.2, 23.7, 22.6, 14.1.

Synthesis of 4,8-bis(5-(9,9-bis(2-ethylhexyl)-9H-fluoren-2-yl)thiophen-2-yl)benzo[1,2-b:4,5-b′]dithiophene(FlT-BDT-EH)

FlT-BDT-EH was synthesized using the similar procedure for FlT-BDT-OC. Yellowish solid (0.82 g, yield: 38%). ^{1}H NMR (300 MHz, $CDCl_3$): δ (ppm) 7.79–7.65 (m, 10H), 7.57–7.48 (m, 6H), 7.41–7.29 (m, 6H), 2.18–1.98 (m, 4H), 1.18–0.68 (m, 24H), 0.66–0.58 (m, 6H). ^{13}C NMR (75 MHz, $CDCl_3$): δ (ppm) 151.5, 150.7, 145.8, 141.2, 140.7, 139.3, 137.8, 136.6, 131.0, 129.2, 127.8, 127.2, 126.8, 124.7, 123.8, 123.3, 123.1, 122.8, 120.1, 120.0, 119.7, 54.9, 44.4, 34.6, 33.6, 28.1, 27.0, 22.8, 14.1, 10.4.

Synthesis of (4,8-bis(5-(9,9-dioctyl-9H-fluoren-2-yl)thiophen-2-yl)benzo[1,2-b:4,5-b′] dithiophene-2,6-diyl)bis(trimethylstannane)(FlT-BDT-OC-Sn)

FlT-BDT-OC (0.22 g, 0.19 mmol) was dissolved in dry THF and the mixture was cooled to −78°C. n-BuLi (2.5 M in hexane) (0.20 mL, 0.48 mmol) was slowly added to the solution and the reaction mixture was stirred for 1 h. And then trimethyltin chloride (0.09 g, 0.42 mmol) in dry THF was added in one portion. The reaction mixture was poured into water and extracted with ether, and dried with Na_2SO_4, filtered, the solvent was removed to obtain yellowish solid, which was further recrystallized to obtain pure product (0.25 g, yield: 87%). ^{1}H NMR (300 MHz, $CDCl_3$): δ (ppm) 7.80–7.66 (m, 10H), 7.59–7.50 (m, 6H), 7.40–7.29 (m, 6H), 2.04–1.93 (m, 8H), 1.29–0.94 (m, 40H), 0.81 (t, 6H), 0.73–0.60 (m, 4H), 0.41 (t, 9H). ^{13}C NMR (75 MHz, $CDCl_3$): δ (ppm) 151.6, 150.9, 146.1, 143.6, 143.0, 141.1, 141.1, 139.5, 137.4, 132.4, 131.0, 129.3, 127.1, 126.8, 124.8, 124.2, 122.9, 122.2, 121.3, 119.9, 119.7, 55.2, 40.4, 31.8, 30.3 29.4, 23.7, 22.6, 14.1,−8.2

Synthesis of (4,8-bis(5-(9,9-bis(2-ethylhexyl)-9H-fluoren-2-yl)thiophen-2-yl)benzo[1,2-b:4,5-b′]dithiophene-2,6-diyl)bis(trimethylstannane) (FlT-BDT-EH-Sn)

FlT-BDT-EH-Sn was synthesized using the similar procedure for FlT-BDT-OC-Sn. Yellowish solid (0.21g, yield: 89%). ^{1}H NMR (300 MHz, $CDCl_3$): δ (ppm) 7.79–7.65 (m, 10H), 7.57–7.48

(m, 6H), 7.41–7.29 (m, 6H), 2.18–1.98 (m, 4H), 1.18–0.68 (m, 24H), 0.66–0.58 (m, 6H), 0.39 (t, 9H). ^{13}C NMR (75 MHz, $CDCl_3$): δ (ppm) 151.3, 150.7, 146.0, 143.4, 142.9, 141.1, 140.8, 139.3, 137.4, 132.4, 131.0, 129.1, 126.9, 126.6, 124.8, 124.1, 122.9, 122.2, 121.3, 120.0, 119.6, 54.9, 44.4, 34.6, 33.6, 28.1, 27.0, 22.8, 14.1, 10.4, −8.2.

General polymerization procedure

P1 and P2 were synthesized by applying microwave-assisted Stille polymerization. The representative procedure for the synthesis of polymer P1 is as follows: To a 10 mL microwave tube, FlT-BDT-OC-Sn (200 mg, 0.14 mmol), DPP (94 mg, 0.14 mmol), $Pd_2(dba)_3$ (2.56 mg, 2 mol%), and P-(o-tolyl)$_3$ (6.82 mg, 16 mol%) were dissolved in anhydrous chlorobenzene. The reaction mixture was purged with N_2 for 20 min. Microwave tube was put into the reactor and heated to 120°C for 45 min. After cooling to room temperature, reaction mixture was poured into methanol to obtain precipitate. The resulting precipitate was purified by Soxhlet extraction method using methanol, acetone, hexane, and chloroform (CF). The CF fraction was evaporated to get P1.

Synthesis of poly [4,8-(bis(5-(9,9-dioctyl-9H-fluoren-2-yl)thiophen-2-yl)benzo[1,2-b:4,5-b′]dithiophene-alt-2,5-diethylhe%)xyl-3,6-bis(5-thiophen-2-yl)pyrrolo[3,4-c]-pyrrole-1,4-dione (P1)

^{1}H NMR (300 MHz, $CDCl_3$): δ (ppm) 7.79–7.60 (m, 12H), 7.58–7.29 (m, 12H), 4.20–4.10 (m, 4H), 2.20–2.00 (m, 8H), 1.30–0.48 (m, 90H). Yield = 0.14 g (61%).

Synthesis of poly [4,8-(bis(5-(9,9-di(2-ethylhexyl)-9H-fluoren-2-yl)thiophen-2-yl)benzo[1,2-b:4,5-b′]dithiophene-alt-2,5-diethylhexyl-3,6-bis(5-thiophen-2-yl)pyrrolo[3,4-c]-pyrrole-1,4-dione (P2)

^{1}H NMR (300 MHz, $CDCl_3$): δ (ppm) 7.79–7.60 (m, 12H), 7.58–7.29 (m, 12H), 4.20–4.10 (m, 4H), 2.20–2.00 (m, 8H), 1.30–0.48 (m, 90H). Yield = 0.16 g (63%).

Fabrication of organic photovoltaic cells

The glass substrates were coated with a transparent ITO electrode (110 nm thick, 10∼15 Ω/sq sheet resistance), which was ultrasonically cleaned with detergent, distilled water, acetone, and isopropyl alcohol. Then, the layer of 40 nm thick PEDOT:PSS (Clevios PVP AI 4083) was spin-coated onto the pre-cleaned and UV-ozone treated ITO substrates and the film baked in air at 140°C for 20 minutes. The solution of active layer, which was prepared by dissolving appropriate ratios of P1:PC_{71}BM in *o*-dichlorobenzene (ODCB) and P2:PC_{71}BM in chlorobenzene (CB), was filtered with 0.45 μm PTFE (hydrophobic) syringe filter and spin-coated on the top of the PEDOT:PSS with the layer thickness of 75∼85 nm, dried at room temperature for 30–40 minute. The lithium fluoride (0.5 nm) and aluminum (Al) cathode (120 nm) were deposited on the top of the active layer under vacuum less than 5.0×10^{-6} torr, which yields a 9 mm^2 of active area per each pixel. The film thickness was measured with a α-Step IQ surface profiler (KLA Tencor, San Jose, CA).The performance of PSCs were measured using a calibrated AM 1.5G solar simulator (Oriel® Sol3A™ Class AAA solar simulator, models 94043A) with a light intensity of 100 mW/cm^2 adjusted using a standard PV reference cell

(2 cm × 2 cm, mono crystalline silicon solar cell, calibrated at NREL, Colorado, USA) and a computer controlled Keithley 2400 source measure unit. The incident photon to current conversion efficiency (IPCE) was measured using Oriel® IQE-200™. While measuring the photocurrent density-voltage (*J-V*) characteristics for PSCs, a black mask was used and only the effective area of the cell was exposed to light irradiation.

Hole mobility

The apparent charge carrier mobility was evaluated from the current *J-V* curves of single charge carrier devices and the results were subsequently fit using the space charge limited current (SCLC) method. In order to measure the SCLC of only one type of charge carrier in a blend, the other one must be suppressed by a large injection barrier, resulting in an electron or hole only device. To measure the hole mobility in P1, P2 devices were made with the structure of ITO/PEDOT:PSS/polymer (P1 or P2) /MoO_3/Al. By taking the current-voltage measurements in the range of 0–3 V and fitting the results to a space charge limited form, where SCLC is described by the Mott-Gurney law[12].

$$J = (9/8)\,\varepsilon_r \varepsilon_0 \mu \left(V^2/L^3\right)$$

Where ε_r is the dielectric constant ($\varepsilon_r = 3$), ε_0 is permittivity of free space, L the thickness of the active layer, μ is the charge mobility and V is the voltage drop across the device ($V = V_{appl} - V_{bi}$, where V_{appl} is the applied voltage to device and V_{bi} is the built-in voltage).

Results and discussion

Synthesis and characterization

Scheme 1 shows the structures of the conjugated polymers with the same polymer backbone and different side chains. DPP was synthesized following the reported literature[13]. The fluorene unit provides a space for introducing two alkyl chains for attaining good solubility for the polymers[14]. From the synthetic point of view, it is easy to introduce alkyl chains on fluorene unit when compared to thiophene unit. Hence, we believe that the attachment of FlT group to the BDT unit in upward and downward directions offer better performance via inexpensive solution processing fabrication conditions. The organization of an electron-rich (donor) and an electron-deficient unit (acceptor) in a polymer main chain is a famous synthetic approach to yield a LBG with rather high charge carrier mobilities, owing to the intramolecular charge transfer. Hence, P1 and P2 were prepared by polymerizing a new FlT-BDT donor moiety with DPP as the acceptor moieties, under microwave-assisted Stille reaction conditions. The resulting polymers were carefully purified through Soxhlet extraction using methanol, acetone, and hexane, to remove the low molecular weight fractions. All polymers exhibited good solubility in common organic solvents, such as THF, CB, ODCB, and CF. The chemical structures of the synthesized monomers and polymers were confirmed by ^{1}H NMR. M_n of P1 and P2 was 20197, 28002 Da with PDI of 1.89 and 1.86, respectively. The disparity in the M_n of the two FlT-BDT based polymers tend to almost same values, because alkyl chain has no affect in molecular weight of polymers. The thermal properties of the two polymers were measured by TGA at a heating rate of 10°C/min and N_2 (Figure 1). The onset of decomposition temperature (T_d, corresponding to 5% weight loss) of P1and P2 was 427, 408°C, respectively, indicating their very high thermal stability.

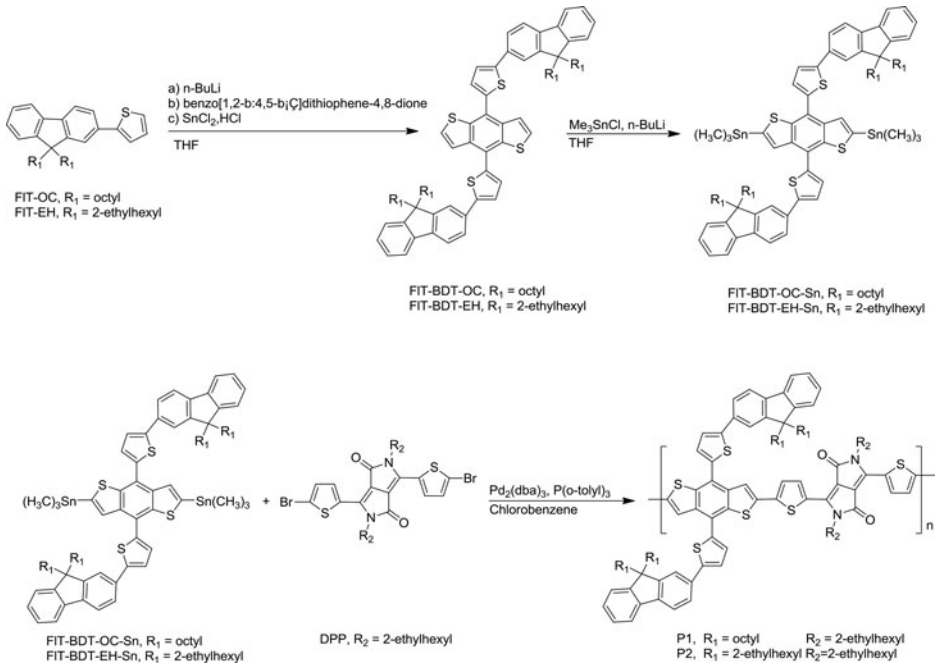

Scheme 1. Synthetic route for **P1** and **P2**.

Optical and electrochemical properties of newly designed FIT-BDT-based polymers

The UV–vis absorption spectra of P1, P2 in CF solution and thin film state are shown in Figure 2. P1 exhibits two well-defined absorption peaks, one at higher energies (300–450 nm) resulting from $\pi-\pi^*$ transitions and the other one at lower energies (500–700 nm). The thin-film absorption of P1 exhibits similar optical property to that in solution[15]. The thin film absorption spectra of P1 and P2 is shown in Figure 2b. From solution state to film state, the maximum absorption peak of P1 was red-shifted by 4 nm, and the intensity of the shoulder peak was increased due to stronger intermolecular interactions in the film state[16]. In addition, obvious vibronic shoulder peaks at lower energies are observed both in solution and thin film, which suggests significant order in the polymer structure. The optical bandgap (E_g^{opt})

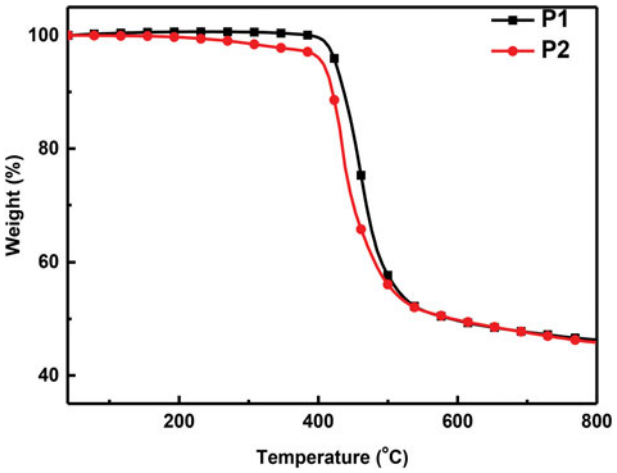

Figure 1. TGA curves of **P1** and **P2**.

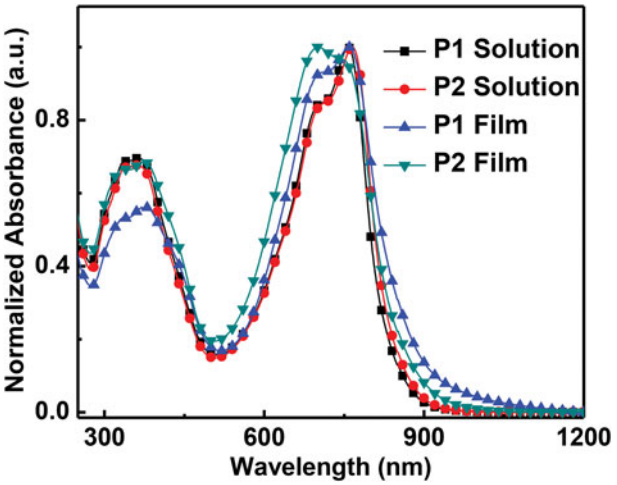

Figure 2. UV-visible absorption spectra of **P1** and **P2** in chloroform solution and film state.

estimated from the film absorption onset is 1.36 eV. The solution spectra of P1 and P2 exhibited a similar trend[17]. As anticipated, P1 and P2 tend to having similar band gap. The E_g^{opt} of P1 and P2 was estimated from the onset absorption edge of the thin film absorption spectra and found to be 1.36 and 1.35 eV, respectively. However, in case of P2 the intensity of vibronic shoulder peak was reduced because of reduced interactions between the side chains in the film state. P1 show stronger $\pi-\pi$ stacking than P2 in film state. Thus, the arrangement of polymer chain in P1 is aligned properly in film state compare to P2, which improves charge transfer. We predict that charge transfer and PCEs will be more for PSCs devices based on P1. The electrochemical properties of FIT-BDT-based polymer films were investigated by CV and the results are shown in Figure 3. Since, both P1 and P2 possess the same conjugated back bone framework, we expect that there would not be much difference in HOMO values. In agreement with our observation, the calculated HOMO values for P1 and P2 were found to be −5.34 and −5.32 eV. It is worth noting that, the variation in alkyl chains has no significant impact on the HOMO levels of the polymers. The HOMO of P1 and P2 are significantly deeper than that of P3HT (−4.76 eV) and close to the ideal HOMO energy level (−5.2 eV), which suggests their high air stability[18]. The LUMO levels are calculated from E_g^{opt} and the HOMO energy levels. The LUMO levels of P1 and P2 were calculated to be −3.98 and −3.97 eV, respectively, as estimated from E_g^{opt} and the HOMO energy levels.

Photovoltaic properties and optimization of newly designed FIT-BDT-based polymers

The BHJ PSCs were fabricated with a configuration of ITO/PEDOT:PSS/P1 or P2:$PC_{71}BM$/LiF/Al and tested under the illumination of AM 1.5G illumination (100 mW/cm^2). In order to get the best device performance, several device and processing conditions such as suitable solvent, polymer to $PC_{71}BM$ ratio, active layer thickness, and processing additive were systematically optimized. The best photovoltaic properties were obtained with the blend ratio of 1:2 for the P1 and P2 devices, respectively. Figure 4a show *J-V* curves of best devices of pristine and additive treated P1 and P2 devices and the data are summarized in Table 1, respectively. The best device of pristine P1 delivered 1.36% of PCE, which is slightly higher than that of the best device of the pristine P2 (PCE: 0.81%) attributed to the higher V_{oc} of 0.78 V, J_{sc} of 4.07 mA/cm^2, and FF of 42.26%. This can be explained from its broad absorption spectrum and higher carrier mobilities of the

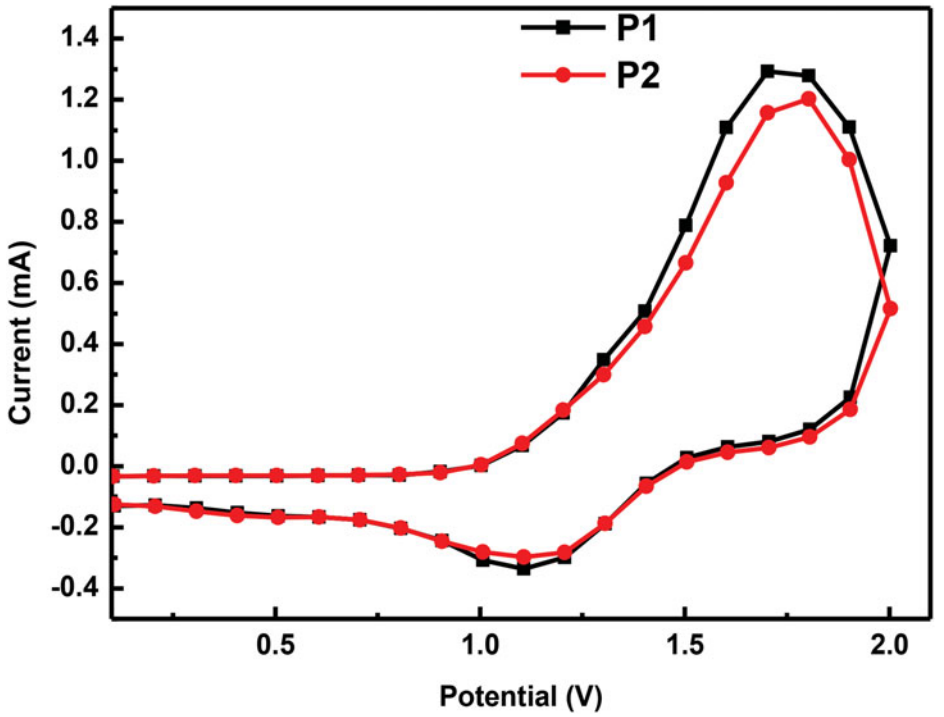

Figure 3. CV curves of **P1** and **P2** thin films.

P1:$PC_{71}BM$ blend than the P2:$PC_{71}BM$ blend. Additionally, the P1 device shows a higher V_{oc} than that of the P2 device due to its slightly deeper HOMO energy level since the V_{oc} mainly depends on the HOMO of the donor and LUMO of the acceptor. Due to the relative higher carrier mobilities of the P1:$PC_{71}BM$ blend, it shows higher FF and J_{sc} values than that of the P2:$PC_{71}BM$ blend, which leads to higher PCE for the P1 device than the P2 device. There have been reports that the FF and J_{sc} of OPV devices could be greatly improved by using additives such as 1,8-diiodooctane (DIO) and chloronaphthalene by forming excellent active layer morphology (Figure 5). To further improve the photovoltaic performance of P1 and P2, an optimal amount of DIO (1 vol%) was introduced. These high boiling additives can adjust the morphology to attain nanoscale phase separation of the polymer:$PC_{71}BM$ blends during spin coating and consequently significant improvement in PCE could be visualized. Surprisingly, interesting observations were recognized after introducing optimum amount (1 vol%) of DIO. Atomic force microscope (AFM) images of the polymer:$PC_{71}BM$ films were taken to compare the surface morphology of the blend films before and after the addition of DIO. The AFM images of polymer:$PC_{71}BM$ and polymer:$PC_{71}BM$ +1% DIO are shown in Figure 5. The root-mean-square (RMS) roughness values of P1 and P2 were found to be 0.4 and 1.2 nm, respectively, whereas after addition of DIO the RMS values of P1 and P2 blend films were slightly decreased to 0.28 and 0.94 nm, respectively. The AFM images revealed that after addition of 1% DIO the morphology of blend films of polymer:$PC_{71}BM$ was adjusted in such a way to attain efficient charge transport to the respective electrodes. Consequently, an improvement in both J_{sc} and FF were observed along with PCE. We observed PCE of 1.78, and 1.20% for the devices of P1, and P2 respectively. The most efficient P1-based device, obtained using 1% DIO, had a PCE of. 1.78%, with J_{sc} of 5.39 mA/cm^2, FF of 43.11%, and V_{oc} of 0.77 V. However, the overall PCE was increased for the devices based on P1, and P2

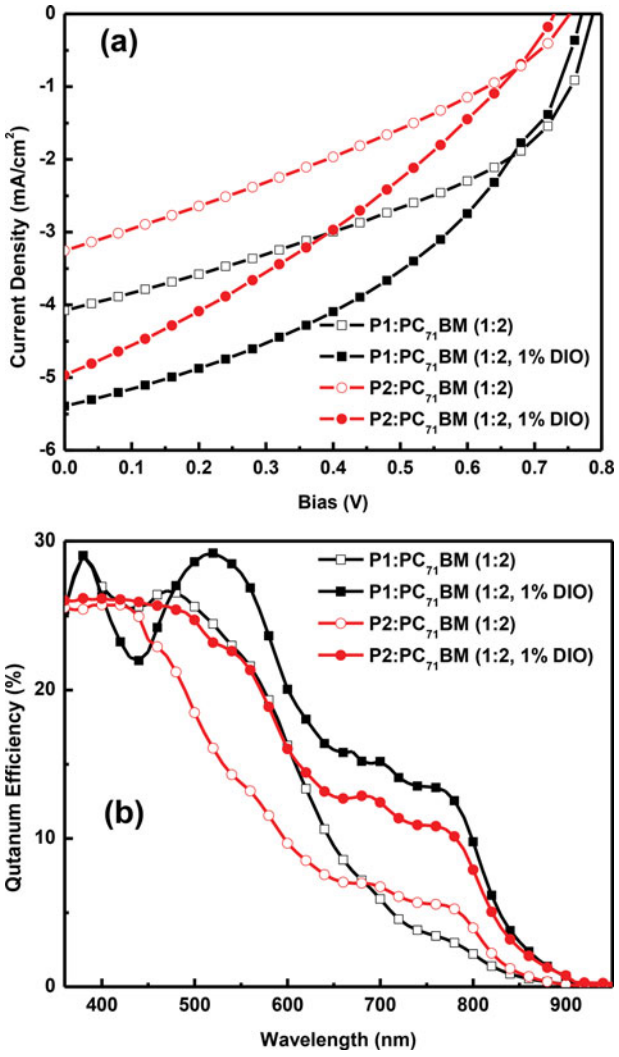

Figure 4. (a) J–V curves and (b) EQE curves of the devices.

after adding 1% DIO. The change of PCEs is primarily due to the improved J_{sc} and slightly improved FF (shown in Table 1). We presume that DIO facilitated the polymer:$PC_{71}BM$ phase separation and increase intermolecular packing to realize high PCE for the OPV devices. We tested the OPV performance of BHJ PSCs by adding more than 1% DIO, but we did not observe any promising results. As shown in Figure 4b, pristine blend of both the polymers covers the external quantum efficiency (EQE) from 300 to 900 nm, which are well matched with their absorption patterns. The improvement in device performance due

Table 1. Summary of the device performances of the fabricated PSCs.

Device	Polymer	Polymer:$PC_{71}BM$	Thickness (nm)	V_{oc} (V)	J_{sc} (mA/cm²)	FF (%)	Hole mobility ($cm^2/V{\cdot}s$)	PCE (%)
1	P1	1:02	75	0.78	4.07	42.26	3.57×10^{-5}	1.36
2	P1	1:2 (DIO 1%)	78	0.77	5.39	43.11		1.78
3	P2	1:02	81	0.75	3.25	32.63	1.93×10^{-5}	0.81
4	P2	1:2 (DIO 1%)	84	0.73	4.96	32.9		1.2

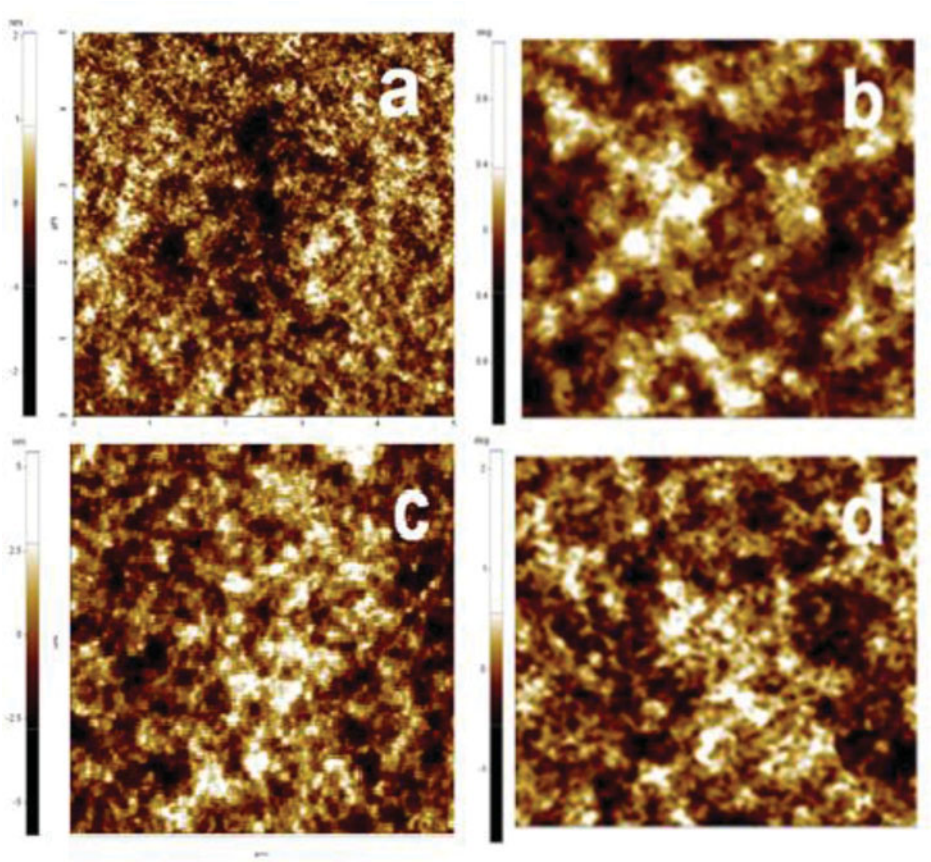

Figure 5. Atomic force microscopy (AFM) images of the blend films of (a) **P1:PC$_{71}$BM**, (b) **P1:PC$_{71}$BM** with 1% DIO, (c) **P2:PC$_{71}$BM**, and (d) **P2:PC$_{71}$BM** with 1% DIO.

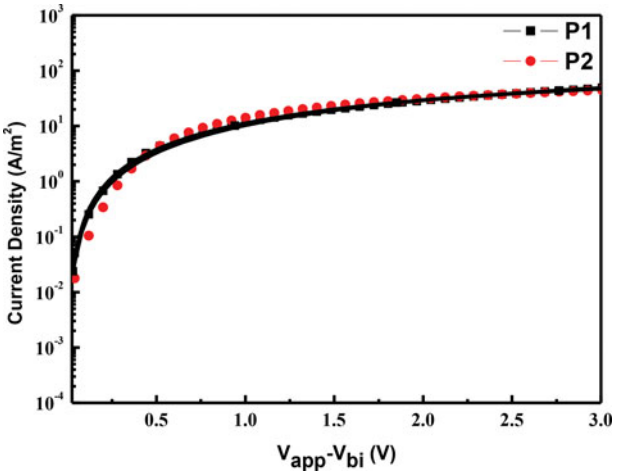

Figure 6. SCLC mobility curves of the holy only devices of **P1** and **P2**.

to addition of DIO additive is also observed from the IPCE spectra of the devices. There is significant broadening of IPCE spectra for device with 1% DIO and with recorded relatively higher value of J_{sc}. The hole mobilities of the two polymers were investigated by the SCLC method. The relationship between current and voltage in the hole-only devices of polymer films is shown in Figure 6. The hole mobilities of P1 and P2 were 3.59×10^{-5} and 1.91×10^{-5} $cm^2/V{\cdot}s$, respectively. All polymer/$PC_{71}BM$ blends showed a relatively low hole mobility which may be one of the reasons for J_{sc} values in OPV devices.

Conclusions

Two LBG polymers, P1 and P2, have been synthesized successfully by introducing FlT as a new conjugated side chain group on BDT unit to comprehend the influence of alkyl chain topology on the $\pi-\pi$ stacking and the photovoltaic properties. The well-resolved and maintained shoulder peak in the thin film compared to solution state is observed between 670 and 720 nm for P1, endorses the efficient $\pi-\pi$ stacking of the polymer backbone. In contrast, the shoulder peak for P2 is reduced in the thin film state when compared to its solution. This indicates that the P1 possess more planar backbone features than that of P2. The best device of P1 showed the maximum PCE of 1.78% with the V_{oc} of 0.77 V whereas the best device of P2 showed the PCE of only 1.20% with the V_{oc} of 0.73 V. This can be understood by the well maintained interactions between the polymer chains due to the linear octyl chains on fluorene unit of FlT conjugated side chain introduced on BDT unit, which lead to increases the carrier mobilities of P1 than P2.

Acknowledgments

This work was supported by grant fund from the National Research Foundation (NRF) (2011-0028320) and the Pioneer Research Center Program through the NRF (2013M3C1A3065522) by the Ministry of Science, ICT & Future Planning (MSIP) of Korea.

References

[1] You, J. B., Dou, L. T., Yoshimura, K., Kato, T., Ohya, K., Moriarty, T., Emery, K., Chen, C.-C., Gao, J., Li, G., Yang, Y. (2013). *Nat Commun.*, *4*, 1446.
[2] Li, G., Zhu, R., Yang, Y. (2012). *Nature Photonics*, *6*, 153.
[3] Dennler, G., Scharber, M.C., Ameri, T., Denk, P., Forberich, K., Waldauf, C., Brabec, C. J. (2008). *Adv. Mater.*, *20*, 579.
[4] Liang, Y., Wu, Y., Feng, D., Tsai, S.-T., Son, H.-J., Li, G., Yu, L. (2009). *J. Am. Chem. Soc.*, *131*, 56.
[5] Thompson, B. C., Fréchet, J. J. M. (2008). *Angew. Chem. Int. Ed.*, *47*, 58.
[6] Chen, J.-D., Cui, C., Li, Y.-Q., Zhou, L., Ou, Q.-D., Li, C., Li, Y., Tang, J.-X. (2015). *Adv. Mater.*, *27*, 1035.
[7] a) Huo, L., Hou, J., Zhang, S., Chen, H,-Y., Yang, Y. (2010). *Angew. Chem. Int. Ed.*, *49*, 1500. b) Huo, L., Zhang, S., Guo, X., Xu, F., Li, Y., Hou, J. (2011). *Angew. Chem.*, *123*, 9871.
[8] Zhang, M., Gu, Y., Guo, X., Liu, F., Zhang, s., Huo, L., Russell, T. P., Hou, J. (2013). *Adv. Mater.*, *25*, 4944.
[9] Schwartz, P.-O., Zaborova, E., Bechara, R., Lévêque, P., Heiser, T., Méry, S., Leclerc, N. (2013). *New J. Chem.*, *37*, 2317.
[10] Yuan, J., Zhai, Z., Dong, H., Li, J., Jiang, Z., Li, Y., Ma, W. (2013). *Adv. Funct. Mater.*, *23*, 885.
[11] Zhang, S., Ye, L., Wang, Q., Li, Z., Guo, X., Huo, L., Fan, H., Hou, J. (2013). *J. Phys. Chem. C.*, *117*, 9550.
[12] Murgatroyd, P. N. (1970). *J. Phys. D: Appl. Phys.*, *3*, 151.

[13] Dou, L., Gao, J., Richard, E., You, J., Chen, C.-C., Cha, K. C., He, Y., Li, G., Yang, Y. (2012). *J. Am. Chem. Soc.*, *134*, 10071.
[14] Meng, B., Song, H., Chen, X., Xie, Z., Liu, J., Wang, L. (2015). *Macromolecules*. *48*, 4357.
[15] Chakravarthi, N., Gunasekar, K., Kim, C. S., Kim, D.-H., Song, M., Park, Y. G., Lee, J. Y., Shin, Y., Kang, I.-N., Jin, S.-H. (2015). *Macromolecules*, *48*, 2454.
[16] Lin, Y., Ma, L., Li, Y., Liu, Y., Zhu, D., Zhan, X. (2014). *Adv. Energy Mater.*, *4*, 1300626.
[17] Yiu, A. T., Beaujuge, P. M., Lee, O. P., Woo, C. H., Toney, M. F., Fréchet, J. M. J. (2012). *J. Am. Chem. Soc.*, *134*, 2180.
[18] Li, Y., Xu, B., Li, H., Cheng, W., Xue, L., Chen, F., Lu, H., Tian, W. (2011). *J. Phys. Chem. C.*, *115*, 2386.